UNIVERSITY OF BIRMINGHAM
University of Birmingham Research at Birmingham

Assessing blending of non-newtonian fluids in static mixers by planar laser- induced fluorescence and electrical resistance tomography

Forte, Giuseppe; Albano, Andrea; Simmons, Mark; Stitt, E. Hugh; Brunazzi, Elisabetta ; Alberini, Federico

DOI:
10.1002/ceat.201800728

License:
Other (please specify with Rights Statement)

Document Version
Peer reviewed version

Citation for published version (Harvard):
Forte, G, Albano, A, Simmons, M, Stitt, EH, Brunazzi, E & Alberini, F 2019, 'Assessing blending of non-newtonian fluids in static mixers by planar laser- induced fluorescence and electrical resistance tomography', *Chemical Engineering & Technology*, vol. 42, no. 8, pp. 1602-1610. https://doi.org/10.1002/ceat.201800728

Link to publication on Research at Birmingham portal

Publisher Rights Statement:
Checked for eligibility: 28/06/2019

This is the peer reviewed version of the following article: Forte, G. , Albano, A. , Simmons, M. J., Stitt, H. E., Brunazzi, E. and Alberini, F. (2019), Assessing Blending of Non-Newtonian Fluids in Static Mixers by Planar Laser-Induced Fluorescence and Electrical Resistance Tomography. Chem. Eng. Technol.. doi:10.1002/ceat.201800728., which has been published in final form at: https://doi.org/10.1002/ceat.201800728. This article may be used for non-commercial purposes in accordance with Wiley Terms and Conditions for Use of Self-Archived Versions.

General rights
Unless a licence is specified above, all rights (including copyright and moral rights) in this document are retained by the authors and/or the copyright holders. The express permission of the copyright holder must be obtained for any use of this material other than for purposes permitted by law.

•Users may freely distribute the URL that is used to identify this publication.
•Users may download and/or print one copy of the publication from the University of Birmingham research portal for the purpose of private study or non-commercial research.
•User may use extracts from the document in line with the concept of ‘fair dealing’ under the Copyright, Designs and Patents Act 1988 (?)
•Users may not further distribute the material nor use it for the purposes of commercial gain.

Where a licence is displayed above, please note the terms and conditions of the licence govern your use of this document.

When citing, please reference the published version.

Take down policy
While the University of Birmingham exercises care and attention in making items available there are rare occasions when an item has been uploaded in error or has been deemed to be commercially or otherwise sensitive.

If you believe that this is the case for this document, please contact UBIRA@lists.bham.ac.uk providing details and we will remove access to the work immediately and investigate.

Download date: 23. Apr. 2024

Assessing blending of non-Newtonian fluids in static mixers by Planar Laser Induced Fluorescence and Electrical Resistance Tomography

G. Forte[1,2], A. Albano[1,3], M.J.H. Simmons[1], E.H. Stitt[2], E. Brunazzi[3], F. Alberini[1*]

[1] School of Chemical Engineering, University of Birmingham, Edgbaston, B152TT, Birmingham, UK.

[2] Johnson Matthey Technology Centre, TS23 4LB, Billingham, UK.

[3] Department of Civil and Industrial Engineering, University of Pisa, I-56126, Pisa, Italy.

*Corresponding author: f.alberini@bham.ac.uk

Abstract: PLIF and ERT have been used simultaneously to monitor the mixing performance of 6 elements KM static mixer for the blending of non-Newtonian fluids of dissimilar rheologies in the laminar regime. The areal distribution method was used to obtain quantitative information from the ERT tomograms and the PLIF images. Comparison of the ERT and PLIF results demonstrates the ability of ERT to detect mixing performance in cases of poor mixing within the resolution of the measurement, though the accuracy decreases as the condition of perfect mixing is approached. ERT thus has the potential to detect poor mixing within the confines of its resolution limit and the required conductivity contrast, providing potential rapid at-line measurement for industrial practitioners.

Keywords: Mixing, Non-Newtonian, ERT, PLIF, Static mixer

Introduction

Non-Newtonian fluids are widespread in industrial processes, for example in the manufacture of home and personal care products, foods and chemicals. Amongst other unit operations, mixing and blending of complex fluids remains a significant process challenge (Connelly and Kokini, 2007; Prakash et al., 1999). Although this operation is often executed in stirred tanks, the industry-driven benefits of moving towards continuous processing suggests a solution involving static mixers. Such devices consist of metallic inserts installed within pipes and applications also include chemical reactions and heat transfer (Paul et al., 2004). Static mixers promote chaotic advection within the flow (Alvarez et al., 1998; Hobbs and Muzzio, 1997; Saatdjian et al., 2012; Wunsch and Bohme, 2000) which contributes significantly to

mixing in the laminar regime, considering the difficulty to reach turbulence for non-Newtonian fluids without excessive amount of power input (Aref, 1984; Le Guer and El Omari, 2012). The flow deformation given by the mixing elements causes the formation of striations and as a result the interfacial surface area is increased, improving the diffusion rate at low Reynolds number (Hobbs and Muzzio, 1997).

Many literature studies have been made of the flow in motionless mixers, employing optical methods as Planar Laser Induced Fluorescence (PLIF) (Alberini et al., 2014a; Arratia and Muzzio, 2004; Ramsay et al., 2016, Faes and Glasmacher, 2008), Particle Image Velocimetry (PIV) (Pianko-Oprych et al., 2009; Stobiac et al., 2014; Szalai et al., 2004) or decolorization measurement techniques (Chandra and Kale, 1992; Li et al., 1997). The application of the reported methods requires both the fluid and the pipelines to be transparent, therefore they are not implementable for opaque fluids. An alternative non-invasive technique applicable for opaque media, Positron Emission Particle Tracking (PEPT), employs the Lagrangian tracking of the 3-D position of a positron emitting tracer particle within the fluid to reconstruct its velocity flow field over time (Edwards et al., 2009) and has been applied both for studies on stirred vessels (Barigou, 2004) and static mixers (Rafiee et al., 2011) for Newtonian and non-Newtonian fluids. Alternatively, to measure the concentration distribution, PET (Positron Emission Tracking) can be used where the position and concentration of a radiotracer is monitored in time (Bell, 2015).

Amongst the many geometries commercially available, Kenics® KM static mixers (Chemineer, USA) are commonly used for academic investigations due to their simple geometry (Avalosse and Crochet, 1997; Rahmani et al., 2005; Rauline et al., 2000; Regner et al., 2006; Wageningen et al., 2004). Some works describe numerical simulations of the mixing performance of non-Newtonian fluids in SMX® (Sulzer) geometry (Peryt-Stawiarska, 2014; Wunsch and Bohme, 2000). However, apart from these few studies, the research focus by means of numerical simulation has remained on blending of non-Newtonian fluids in stirred vessels, with the use of different approaches such as Computational Fluid Dynamics including Direct Numerical Simulation (DNS) of the Navier-Stokes equations (Zalc et al., 2002).

The industry driver for continuous processing, is concomitant with the requirement for appropriate Process Analytical Technology (PAT) to enable real-time product quality assurance and control (Uendey et al., 2010). In the context of this paper, the development of in situ measurement techniques represents a critical step towards this. Furthermore, traditional approaches to the development of new formulated liquid products are laboratory scale oriented with little or even no attention given to formulation “manufacturability”. This

frequently results in not only longer and costlier time to scale up but also increased production costs.

A number of measurement techniques have been applied for monitoring fluid characteristics in inline flows. Nuclear Magnetic Resonance (NMR) (Blythe et al., 2017) and ultrasonics (Pfund et al., 2006) were applied to estimate rheological parameters of non-Newtonian fluids (aqueous solutions of Carbopol 940 and Carbopol EZ-1 respectively) in pipelines in real time, while micro-PIV was applied in determining the velocity profile of both non-Newtonian and Newtonian fluids in laminar regime (Fu et al., 2016).

Electrical Resistance Tomography (ERT), amongst other techniques, offers the advantages of being non-invasive, low-cost, robust and with a high temporal resolution; it is thus an interesting candidate technique in this context for measurement of the phase distribution within liquid continuous mixtures (Pakzad et al., 2008; Wang et al., 1999). Jegatheeswaran et al. (2018) uses ERT to validate CFD simulations of the blending of two non-Newtonian fluids flowing in SMX static mixers. The same technique has been used for measuring velocity profiles of shampoo in pipelines (Ren et al., 2017) and to evaluate mixing of industrial pulp in static mixers (Yenjaichon et al., 2011). Recent applications of ERT in pipe flows have demonstrated potential for in-line rheometry measurements (ERR) (Machin et al., 2018).

In this paper, we describe the use of ERT to determine the distribution of two non-Newtonian fluids of dissimilar rheology at the outlet of a Kenics KM static mixer in the laminar regime. The measurements are made at the mixer outlet using a two plane circular array. The ERT measurements are compared with measurements of the mixing distribution collected simultaneously using Planar Laser Induced Fluorescence (PLIF) a proven method in this application. Both ERT and PLIF data are compared quantitatively using the areal distribution method developed by Alberini et al. (Alberini et al., 2014b).

Material and Methods

Aqueous solutions of carboxymethylcellulose (CMC) and Carbopol 940 were chosen as the model of non-Newtonian fluids, whose flow rheology can be well represented by the power law and Herschel Bulkley constitutive laws respectively. Flow curves were obtained and fitted to the constitutive models using a rheometer (TA Instruments, model: Discovery HR-1) equipped with a 40 mm 4° cone and plate geometry and associated software: the data are shown in Tab. 1.

Fig. 1 shows the rig schematic. The flow to the mixer was delivered by an Albany rotary gear pump controlled using an inverter control WEG (model CF208). The secondary flow, doped with fluorescent dye (Rhodamine 6G) with a concentration of 0.04 mg l^{-1} (concentration was

selected within the linear range of greyscale versus dye concentration), was introduced using a Cole-Parmer Micropump (GB-P35). The injection pipe (with internal diameter of 7.6 mm) was placed in the centre of the main pipe as close as possible to the static mixer. The experiments, reported in Tab. 2, were conducted at isokinetic condition between main flow (MF) and secondary flow (SF): the two fluids were fed at the same superficial velocity, u_S, hence the ratio between the two volumetric flows was equal to the ratio between main and injection pipe sections (MF/SF≈10). The Kenics KM mixer unit had an internal diameter of 25.4 mm (1") and length of 220 mm (L/D= 9) and was equipped with 6 mixing elements.

Tab. 1: Fluid rheology parameters.

Fluids	**Mass composition**	**Behaviour**	**τ_0 [Pa]**	**K [Pa/s^n]**	**n [−]**
PL	0.5% w/w sodium Carboxymethyl Cellulose 99.5% w/w water	Power Law		0.49	0.59
HB1	0.1% w/w Carbopol 99.9% w/w water	Herschel-Bulkley	0.85	0.40	0.58
HB2	0.2% Carbopol 99.8% w/w water	Herschel-Bulkley	10.27	7.45	0.38

The mixing unit is followed by a planar circular ERT sensor consisting of 16 electrodes. The ERT sensor was connected to a V5R data acquisition system (Industrial Tomography Systems plc, UK) that controlled electrical excitation and measurement collection. The ERT plane was located 100 mm after the mixer outlet, while the PLIF measurement plane was located at 200 mm from the end of the mixing zone; the two measurement planes were separated by 100 mm.

The terminal part of the pipeline was equipped with a Tee piece designed with a glass window inserted at its end corner through which PLIF measurements are made (the capture procedure may be found in Alberini et al. (2014b).

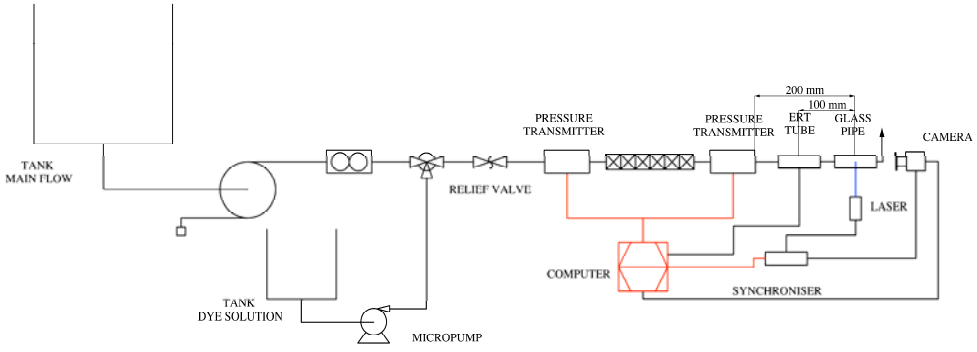

Fig. 1: Schematic of the experimental rig (adapted from Alberini et al. (2014b)) .

A range of superficial velocities, u_S, was investigated to identify the accuracy of ERT measurements once the contrast, in term of conductivity, between the injected (secondary) and the main flow is decreased. The list of experiment and flow conditions is shown in Tab. 2. Within the range of investigated velocities, the values of *Re,* calculated using same methodology used by Alberini et al. (2014a), were in the range 25-220 which suggest the system was always running in laminar regime (*Re* << 2000). The inlet absolute difference in conductivity (no addition of salt), $\Delta c = |c_{MF} - c_{SF}|$, between the main flow (MF) and the secondary flow (SF) is also reported in Tab. 2, since it is the principal parameter which affects the ERT measurement.

Tab. 2: List of experiment and flow conditions.

Experiment	**MF**	**SF**	**Δc (mS cm^{-1})**	**u_S (m s^{-1})**
I	HB1	PL	0.871	0.20 | 0.27 | 0.34 | 0.40 | 0.47
II	HB2	PL	0.686	0.20 | 0.27 | 0.34 | 0.40 | 0.47
III	HB1	HB2	0.112	0.20 | 0.27 | 0.34 | 0.40 | 0.47

Calibration and Post Processing

The ERT system was calibrated prior to the experiment, which consists of taking a baseline reference frame. For each experiment, the reference was captured with continuous phase at each flow rate after reaching a steady flow condition. The V5R automatically sets the conductivity of the reference measurements equal to unity, thus the changes occurring after the injection are relative and not absolute. The V5R system employs a sample frequency of 125 Hz: for each run a sample of 1000 frames was analysed. The data obtained were processed using the Toolsuite V7.4 software (ITS Ltd.) in order to reconstruct conductivity tomograms. Since ERT is a soft-field technique, the reconstruction problem is not trivial and several algorithms have been developed to generate conductivity tomograms from the raw data, both iterative and non-iterative (Yang and Peng, 2003). Commonly, in the latter category, the Linear Back Projection (LBP) method or one of its variants is used (Noser, Tikhonov reconstruction algorithms) (Wei et al., 2015). In this work the modified standard back projection (MSBP) algorithm implemented in the V5r software was used. Furthermore,

for simplicity, only the tomograms obtained in the second plane are used for comparison with PLIF.

The areal method (Alberini et al., 2014b) requires an initial calibration step to be applied in evaluating mixing performance. In this step, the values of C_{inf} and G_{inf} are identified for all the mixtures, as the value of conductivity and greyscale respectively reached at the condition of perfect mixing. Since ERT and PLIF have a different basis of measurement, two dimensionless parameters, X_C and X_G, are introduced to allow comparison of the measured mixing performance between them. A dimensionless relative conductivity X_C can be defined for each pixel as:

$$X_C = (C_i - C_0)/(C_{inf} - C_0) \quad (1)$$

Where C_i is the relative conductivity of the *i*-th pixel of the tomogram, C_{inf} is the relative conductivity achieved at perfect mixing and C_0 is the reference conductivity of the pixel before the injection, equal to 1 in condition of single phase. Analogously, a dimensionless greyscale X_G is defined:

$$X_G = (G_i - G_0)/(G_{inf} - G_0) \quad (2)$$

Where G_i is the grey scale value of the *i*-th pixel of the PLIF image, G_{inf} is the grey scale value reached at perfect mixing found in the calibration step, and G_0 is the reference status of the pixel before the injection. The grey scale values of "pure" (100% secondary flow fluids) fluids have been measured resulting in 92 and 250 for PL and HB2 respectively at fixed Rhodamine 6G concentration of 0.04 mg l^{-1}.

In the calibration procedure, both greyscale values and conductivity of the mixtures are measured at different volume fraction x_{SF} values of the secondary flow in the main flow in the interval of interest. Pre-fully-mixed solutions with volume fractions x_{SF} of the secondary flow between 0.02 and 0.10 (which is the maximum volume ratio obtained in the system), were fed to the system and ERT and PLIF measurements were captured simultaneously. It was noticed that the effect of flow velocity on both measurements (in case of fully premixed solutions) is negligible. The results of the calibration for the relative conductivity and the greyscale values, to obtain C_{inf} and G_{inf}, are reported for the three mixtures in Tab.3.

Tab. 3: Relative conductivity, C_{inf}, and greyscale, G_{inf}, values of the mixture of primary and secondary fluids at different volume fraction of secondary fluids for each pair of fluids employed in the different experiments: I(PL in HB1), II (PL in HB2), and III (HB2 in HB1)

Experiment I		***Experiment II***		***Experiment III***	
x_{pl} **in HB1**	C_{inf}	x_{pl} **in HB2**	C_{inf}	x_{hb2} **in HB1**	C_{inf}
0.02	1.08	0.02	1.06	0.02	0.99
0.04	1.12	0.04	1.10	0.04	0.98
0.06	1.18	0.06	1.13	0.06	0.97
0.08	1.27	0.08	1.15	0.08	0.96
0.1	1.35	0.1	1.18	0.1	0.95
x_{pl} **in HB1**	G_{inf}	x_{pl} **in HB2**	G_{inf}	x_{hb2} **in HB1**	G_{inf}
0.02	120	0.02	247	0.02	247
0.04	119	0.04	243	0.04	245
0.06	119	0.06	240	0.06	242
0.08	118	0.08	237	0.08	239
0.1	118	0.1	234	0.1	237

Results

The two imaging techniques employed have a substantial difference in spatial resolution: whilst PLIF is able to capture high resolution pictures (2048×2048 pixels), ERT yields relatively low resolution tomograms (20×20 pixels) which cannot be expected to resolve striations of fluid that are often present when mixing complex rheology fluids. The first step of the conducted study consists in evaluating the effect of downscaling PLIF images from full resolution to a reduced resolution, of the same order of magnitude of ERT tomograms (32×32 pixels). The applied downsizing algorithm allows a reduction scaled by powers of 2, therefore from the starting resolution of $2^{11}\times2^{11}$ pixels, a resolution of $2^5\times2^5$ pixels is obtained, reasonably close to the ERT tomogram resolution, to draw significant comparison. Subsequently, full size PLIF images and ERT tomograms are directly compared on evaluating achieved mixing performance.

PLIF image analysis by varying resolution

Downscaled PLIF (32×32) images are obtained using the Lanczos kernel downsizing method (Komzsik, 2003) and compared to original full size PLIF images. The objective is to gather

whether at low resolution it is possible to characterize mixing performance and assess the loss of information in downscaling PLIF images. An example of the resulting images are shown in Fig. 2, as a function of flow rate.

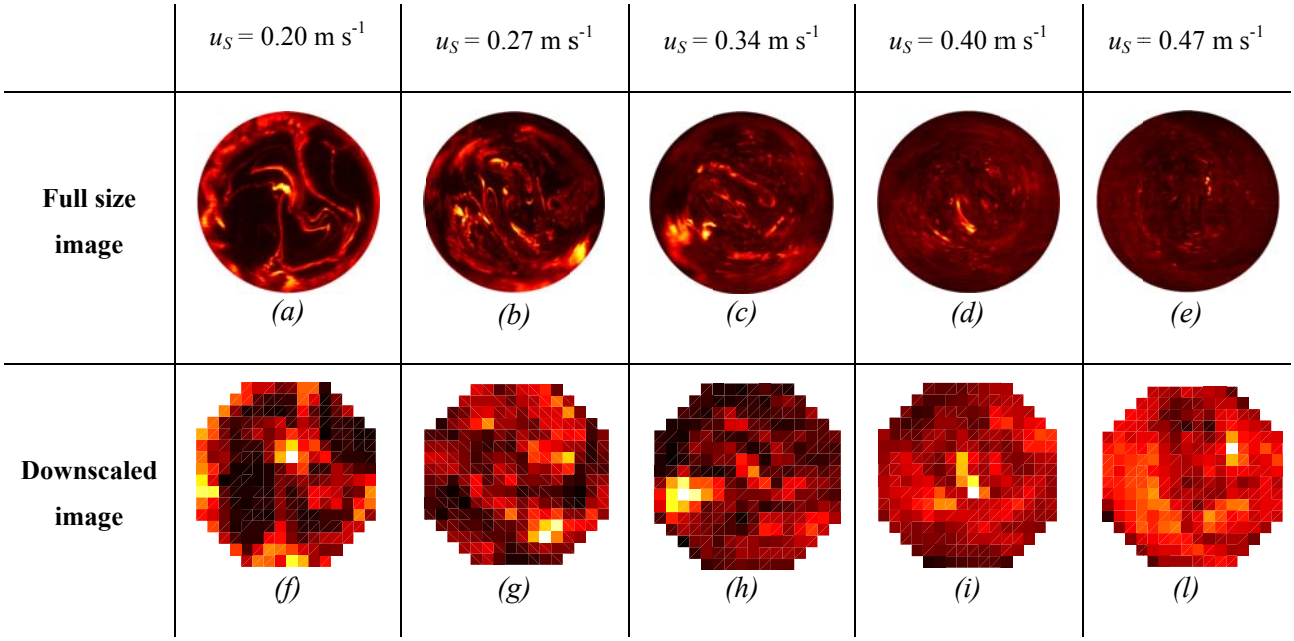

Fig. 2. Full size (a-e) and downscaled (f-l) PLIF images at different superficial velocities for experiment I

In Fig. 2, the thick white striations represent the unmixed secondary flow and the dark areas the main flow. The images show a substantial increase in homogeneity as the flow rate is increased with the dark regions observable in Fig. 2a reducing and the white regions becoming less intense in Fig. 2d and 2e. In an analogous way, the white and black pixels observed in Fig. 2f progressively disappear as u_S increases in Fig. 2l where the image shows improvements in terms of mixing performance.

Although it is possible to appreciate by eye how the downscaling decreases the quality of the images, this transformation does not translate in significant loss of information from a point of view of mixing performance detection capability. In fact, by applying the areal fraction method, it is possible to compare the mixing performance detected by the full resolution pictures and the downscaled images in Fig. 3.

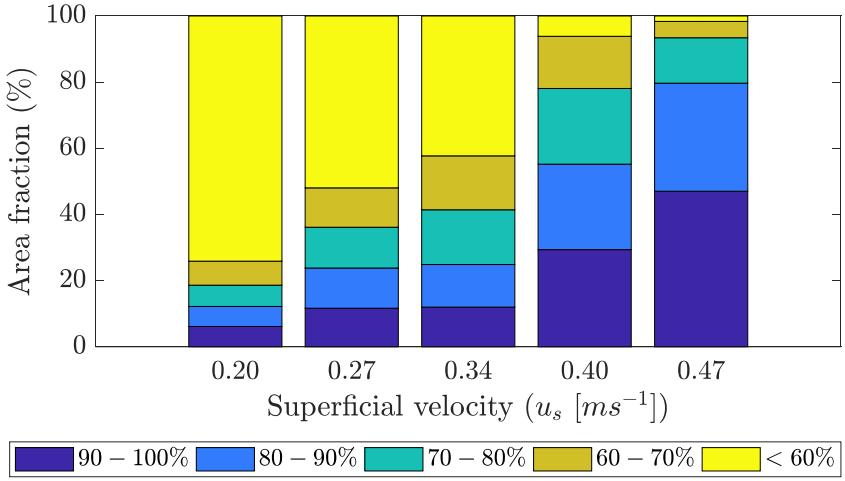

(a)

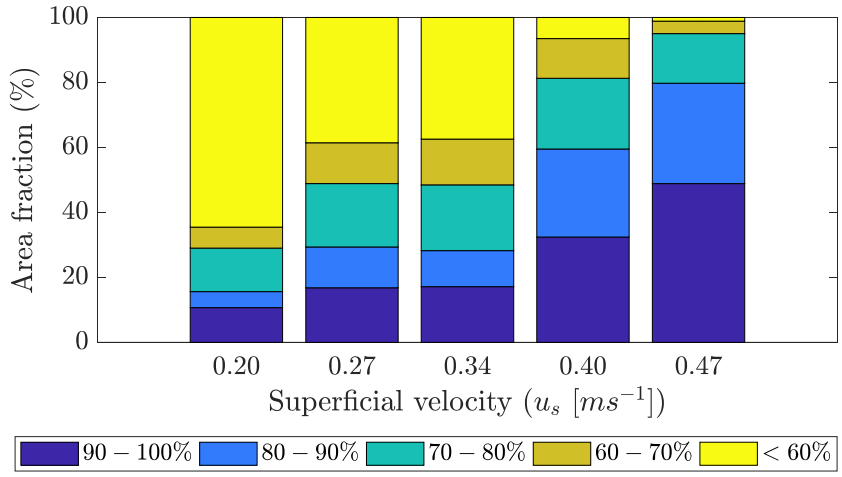

(b)

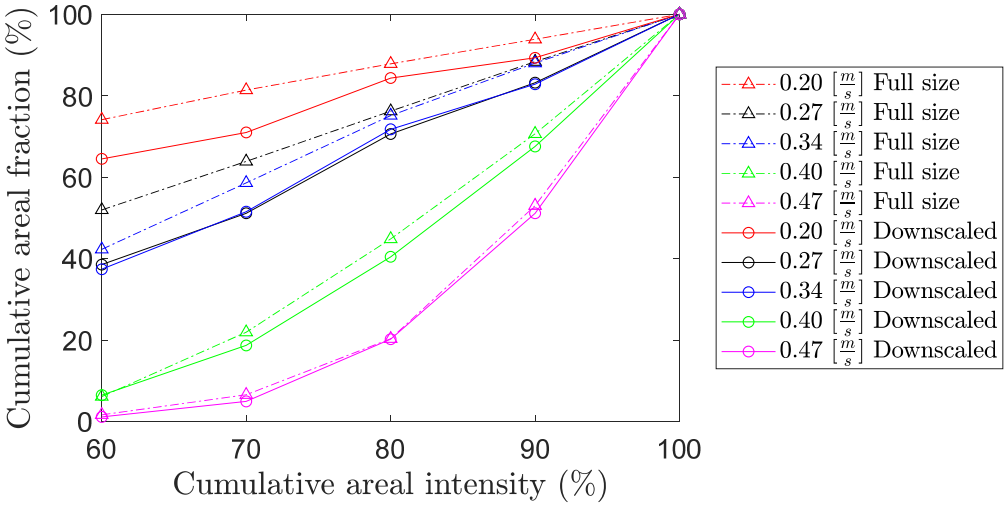

(c)

Fig. 3. Areal fraction performance for full resolution images (a) and downscaled images (b); (c) cumulative distributions of areal intensity

In Fig. 3a and 3b, the area fraction histograms are shown for selected superficial velocities. The mixing performance trends are similar for the two set of data (high resolution in Fig. 3a

and low resolution in Fig. 3b). This suggests that the resolution can affect the overall results but not drastically as it could be expected (see Fig. 3c for the comparison).

The loss of information in this transformation is not significant particularly at high superficial velocity, where the mixing behaviour of the system is equally depicted by the 32×32 and the 2048×2048 images. This analysis demonstrates how in case of optical methods, although higher resolution guarantees a higher level of insight and information at meso and micro scale, it is still possible to gather information on general mixing performance with low resolution images. In the following sections, PLIF is used to evaluate the capability of ERT to describe mixing performance in the pipeline; as in this work, PLIF is used as a validation for ERT, full resolution PLIF images are used for comparison.

ERT-PLIF comparison

Experiment I

Fluids HB1 and PL have similar rheological parameters in terms of consistency index (K) 0.40 and 0.49 and power index (n) 0.58 and 0.59 respectively. The main difference is the presence of a yield stress in HB1. For this set of experiments, different superficial velocities (u_S) were used as given in Tab. 2 and samples of raw PLIF images and ERT tomograms obtained are shown in Fig. 4.

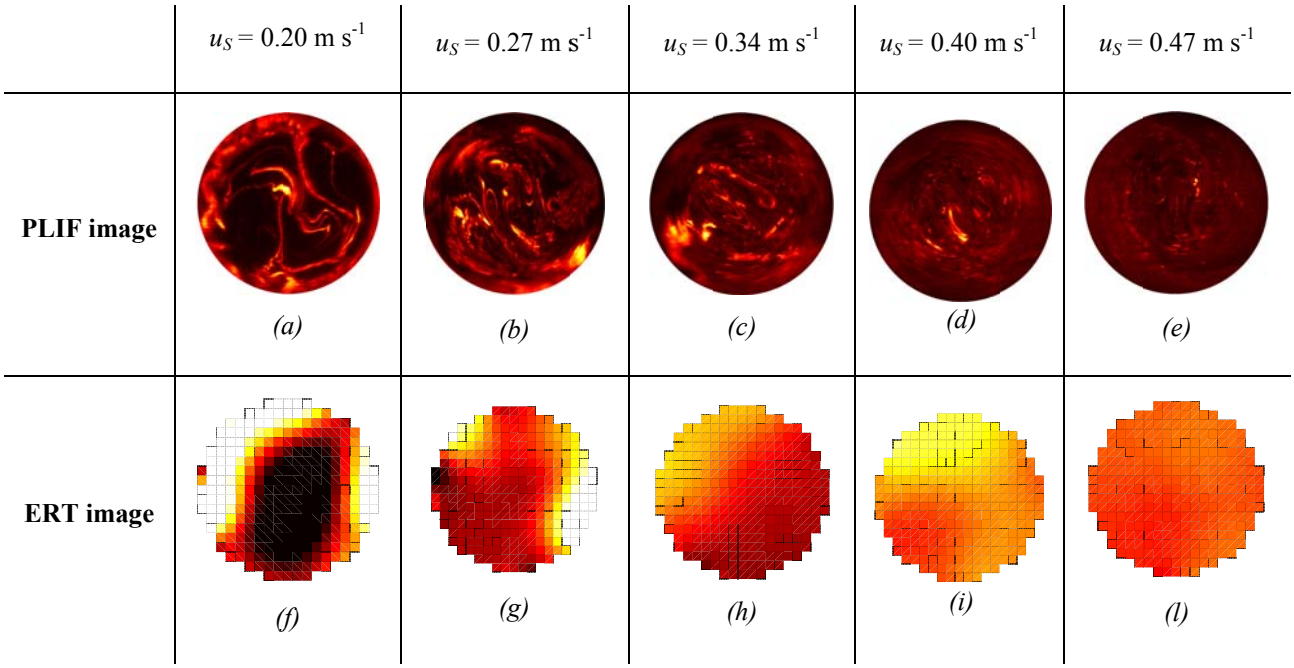

Fig. 4. Full size PLIF (a-e) and ERT (f-l) images at different superficial velocities for experiment I

It should be noted that there is a difference in orientation between the tomogram and the PLIF images since the high conductivity zones in some cases do not correspond to the same location in the PLIF images. This is thought due to residual rotational flow following the KM mixer elements which slowly dissipates after the mixer outlet. As expected, the resolution of the ERT is inferior to the PLIF, yet the contrast in the image is sufficient to identify an unmixed state. In both sets of images, it is possible to appreciate how the uniformity in colour increases as the superficial velocity is increased and better blending is achieved. The areal distribution analysis together with the cumulative plot is shown for both PLIF and ERT measurements for all values of u_S in Fig. 5.

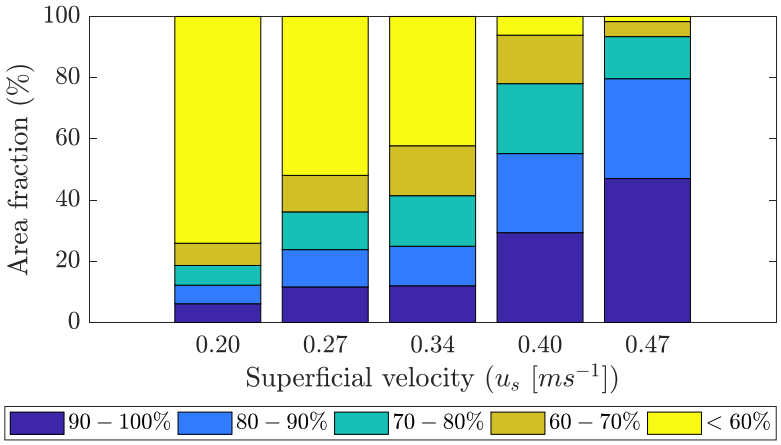

(a)

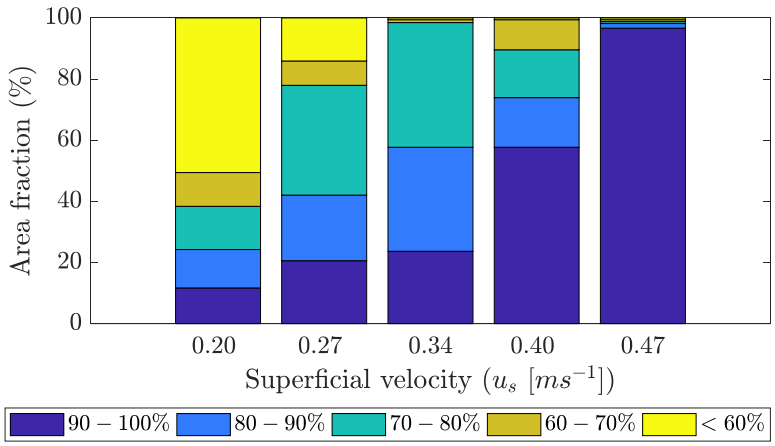

(b)

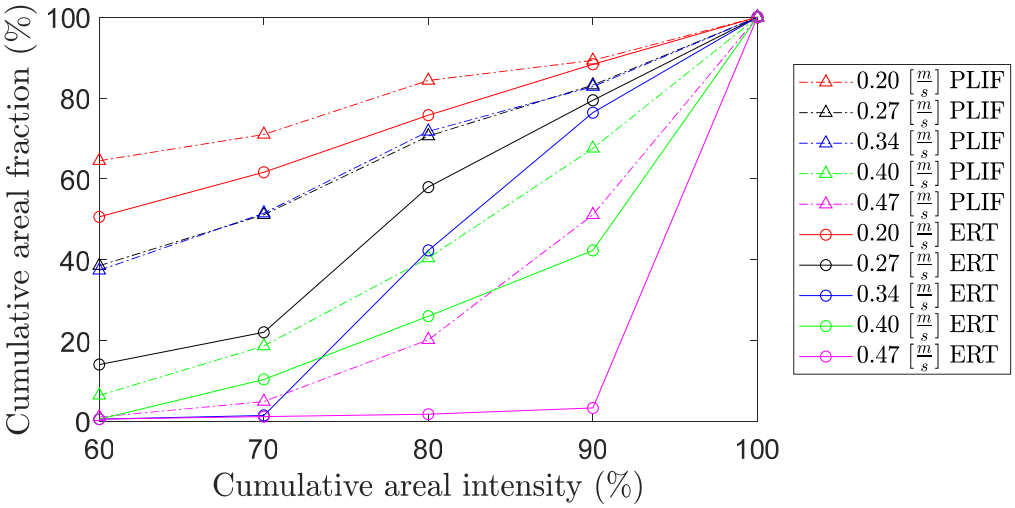

(c)

Fig. 5. Discrete areal intensity distribution from PLIF (a) and ERT (b) for all values of u_S and cumulative distributions of areal intensity comparison (c) for experiment I

As expected, the results do not overlap perfectly due to the different principle and resolution between the two techniques and ERT performs poorly as the mixing improves beyond the

resolution of the measurement and the striations become too thin to be detected. However, for the first four investigated values of u_S, the observed trend of mixing performance is similar. This is taken to extremes at higher speeds, where ERT tomograms overestimate the mixing performance, probably also due to the low contrast between the conductivities of the two mixing fluids, which is a consequence of the reconstructive algorithm.

Experiment II

With the objective to investigate worse mixing performance, a higher concentration of Carbopol 940 was used in the main flow (fluid HB2). As a consequence, the yield stress and the consistency index (K_{HB2}/K_{HB1}~20) values of the secondary fluid, employed in experiment II (PL), are higher. A few examples of PLIF and ERT images are showed in Fig. 6a-e and 6f-l respectively. From previous findings (Alberini et al., 2014b), increasing the viscous properties would be expected to cause a drastic reduction in mixing performance and this is indeed observed - the increase of yield stress entails the formation of lumps as shown in Fig. 6.

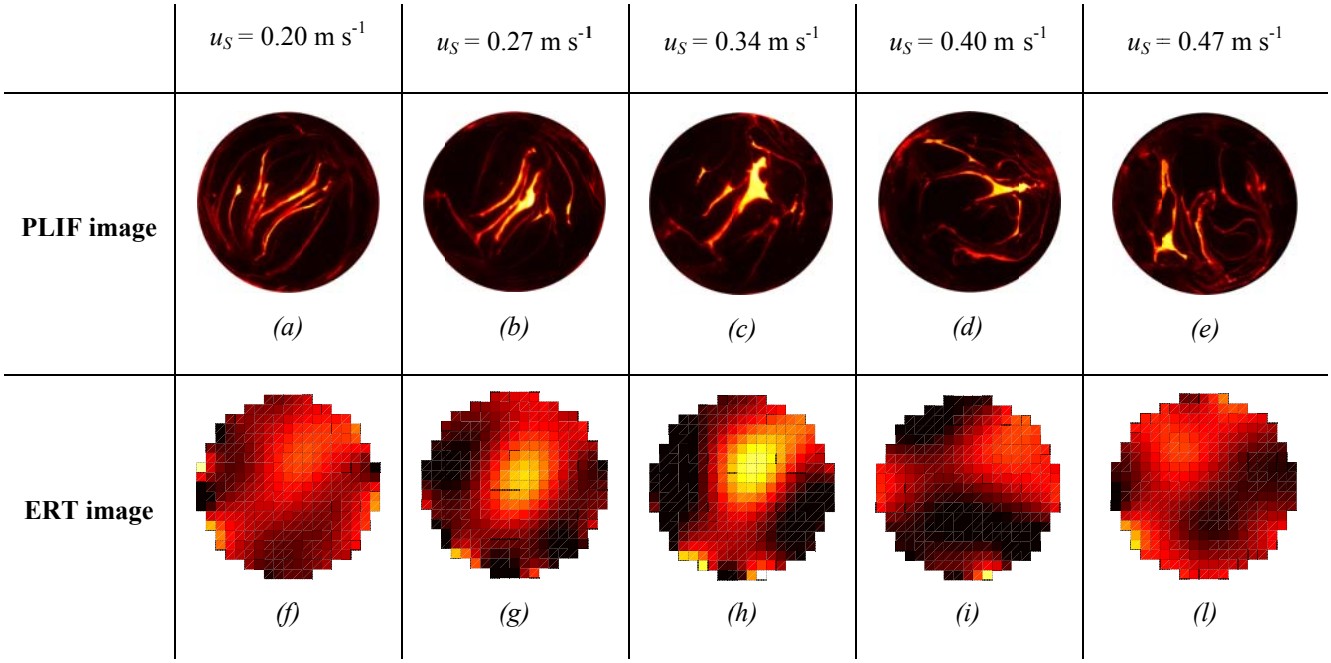

Fig. 6. Full size PLIF (a-e) and ERT (f-l) images at different superficial velocities for experiment II

Both from ERT tomograms and PLIF images it is difficult to qualitatively observe evolutions in mixing performance at higher speed; particularly looking at PLIF images it can be argued that at u_S between 0.27 m s^{-1} (Fig. 6b) and 0.47 m s^{-1} (Fig 6e) the blending does not improve. Despite the ERT tomograms in Fig. 6 are qualitatively well representing the PLIF image, the quantitative agreement shown in the cumulative distribution plot (Fig. 7) is worse.

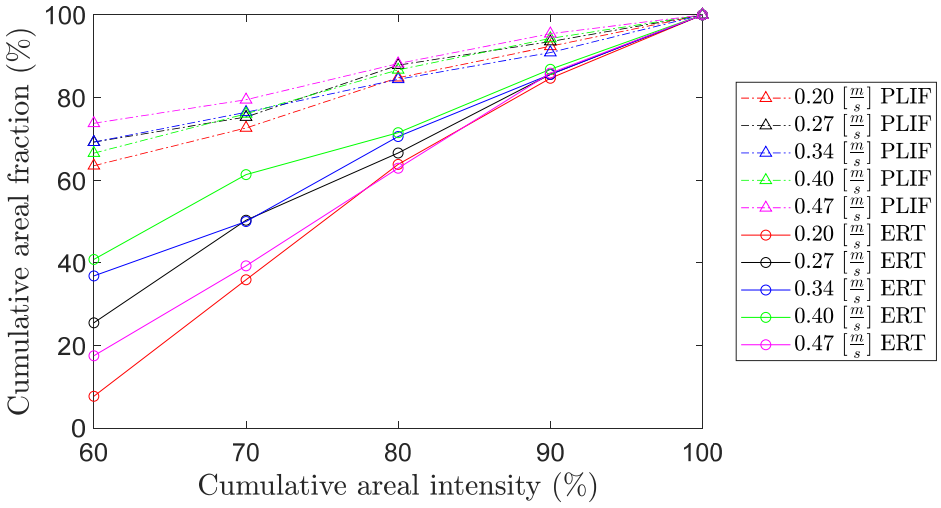

Fig. 7. Cumulative distributions of areal intensity for experiment II

Although, in this case, the ERT is shown to significantly over predict the mixing performance in absolute terms. However, it correctly does not predict an improvement in mixing performance as the superficial velocity is increased. As observed for PLIF, particularly in the high mixing performance categories (90-100 and 80-90%) the system does not record any significant difference between the runs, as shown by the coinciding last three points of the cumulative areal fraction (Fig. 7), meaning that in this case the increase in speed does not significantly improve mixing. This suggests that ERT may be used as a relative measure more than as absolute measurement.

Experiment III

In this experiment, the difference in conductivity was set to a lower value to further challenge the ERT technique. Moreover, at the same time, the level of achieved final mixing is reduced using fluids HB1 and HB2 as the main and secondary flows respectively. In Fig. 8 both instantaneous PLIF images and a ERT tomograms are shown for comparison at different superficial velocities.

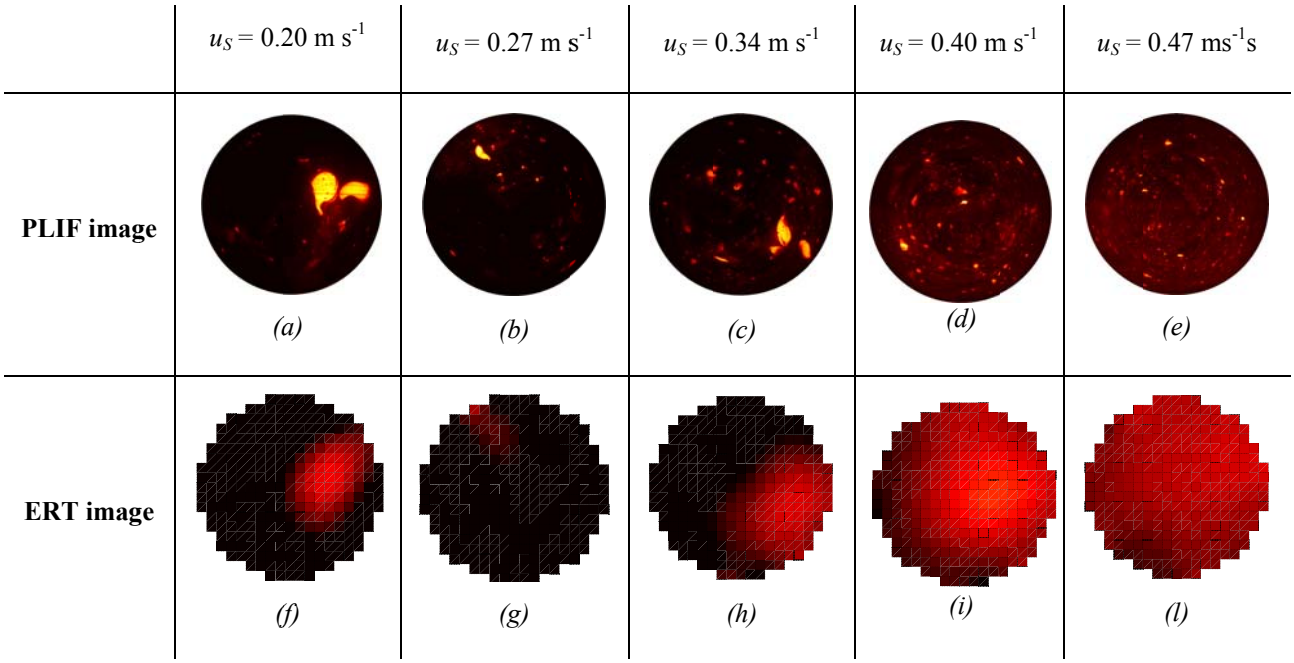

Fig. 8. Full size PLIF (a-e) and ERT (f-l) images at different superficial velocities for experiment III

From PLIF images it is possible to infer that from an unmixed condition at low speeds (Fig. 8a-c) the system moves towards better blending performance once u_S of 0.4 m s^{-1} is reached. The decreased conductivity contrast results in a smaller colour contrast between the secondary and the main phase in ERT tomograms although a higher level of uniformity is achieved at higher speeds.

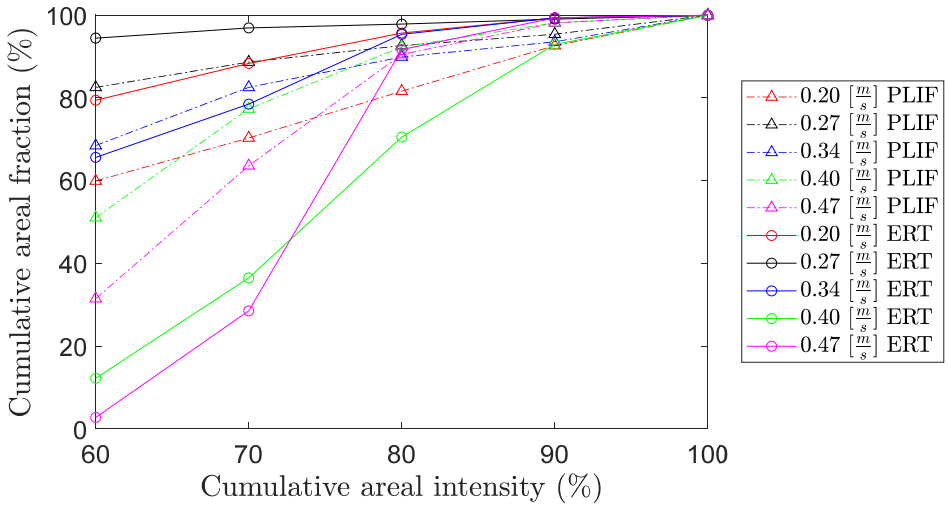

Fig. 9. Cumulative distributions of areal intensity for experiment III

Looking at areal fraction analysis (Fig. 9) it emerges how ERT is able to estimate the unmixed condition at low speed despite the low conductivity contrast. ERT performance still

follows observed trends for PLIF, highlighting the same inflection at mixing performance at the speed of 0.27 m s^{-1}, compared to higher and lower superficial velocities. Although, an overestimation is still observed at high speed, particularly for the category of 70-80% mixing, while in this case ERT does not overestimate the highest mixing condition (80-90% and 90-100%) commonly the targeted condition in mixing processes.

Increasing the speed (above 0.27 m s^{-1}), and as a consequence the number of lumps of unmixed injected material, the divergence between PLIF and ERT data increases consistently. This is an issue which is partly due to the reconstruction algorithm and partly to the measurement resolution. In fact, the first approximates a non-linear problem with a linear hypothesis, instead the low resolution characterising the technique limits the size of lumps that can be detected. Clearly, from the tomograms at low speed (at 0.20 m s^{-1} , 0.27 m s^{-1} and 0.34 m s^{-1}), the lumps, or the agglomerations of lumps, can be detected while at higher speed ERT fails in detecting them. In the present study, an additional obstacle is represented by the use of small conductivity contrast between the employed phases, which however does not seem to affect significantly the measurement in condition of poor mixing.

Conclusions

In this work, the ability of ERT to assess the mixing performance of non-Newtonian fluids in static mixer has been investigated. The same methodology, developed in previous works (Alberini et al., 2014b, 2014a) is used for both PLIF images and ERT tomograms. Three experiments using different fluids with different initial contrast in conductivity have been employed. PLIF has been used to validate the data obtained in terms of qualitative and quantitative analysis. With the proposed method, ERT can be used as a relative measurement (measuring how much the mixing improved relative to the other runs at different superficial velocities) but not as an absolute one, as it could be expected, due to its limitations such as resolution and reconstructive algorithm smoothing. However, the relative trends show high level of agreement with PLIF results in particular to identify conditions of poor mixing (generally for all experimental runs below 0.34 m s^{-1}). This is not the case once the level of mixing increases (generally for all experimental runs above 0.34 m s^{-1}). The tested conditions were inherently challenging for the ERT, considering the employed small conductivity contrast (down to 0.1 mS cm^{-1}), however the lowest observed performance were (commonly to all experiments) obtained when the dimension of the striations/lumps is below the measurement resolution, regardless of the conductivity difference between the mixed phases.

References

Alberini, F., Simmons, M.J.H., Ingram, A., Stitt, E.H., 2014a. Use of an Areal Distribution of Mixing Intensity to Describe Blending of Non-Newtonian Fluids in a Kenics KM Static Mixer Using PLIF. Aiche J. 60, 332–342. https://doi.org/10.1002/aic.14237

Alberini, F., Simmons, M.J.H., Ingram, A., Stitt, E.H., 2014b. Assessment of different methods of analysis to characterise the mixing of shear-thinning fluids in a Kenics KM static mixer using PLIF. Chem. Eng. Sci. 112, 152–169. https://doi.org/10.1016/j.ces.2014.03.022

Alvarez, M.M., Muzzio, F.J., Cerbelli, S., Adrover, A., Giona, M., 1998. Self-similar spatiotemporal structure of intermaterial boundaries in chaotic flows. Phys. Rev. Lett. 81, 3395–3398. https://doi.org/10.1103/PhysRevLett.81.3395

Aref, H., 1984. Stirring by Chaotic Advection. J. Fluid Mech. 143, 1–21. https://doi.org/10.1017/S0022112084001233

Arratia, P.E., Muzzio, F.J., 2004. Planar Laser-Induced Fluorescence Method for Analysis of Mixing in Laminar Flows. Ind. Eng. Chem. Res. 43, 6557–6568. https://doi.org/10.1021/ie049838b

Avalosse, T., Crochet, M.J., 1997. Finite-element simulation of mixing: 2. Three-dimensional flow through a kenics mixer. AIChE J. 43, 588–597. https://doi.org/10.1002/aic.690430304

Barigou, M., 2004. Particle Tracking in Opaque Mixing Systems: An Overview of the Capabilities of PET and PEPT. Chem. Eng. Res. Des., In Honour of Professor Alvin W. Nienow 82, 1258–1267. https://doi.org/10.1205/cerd.82.9.1258.44160

Bell, S.D., 2015. The Development of Radioactive Gas Imaging for the Study of Chemical Flow Processes. PhD Thesis, University of Birmingham, Birmingham.

Blythe, T.W., Sederman, A.J., Stitt, E.H., York, A.P.E., Gladden, L.F., 2017. PFG NMR and Bayesian analysis to characterise non-Newtonian fluids. J. Magn. Reson. 274, 103–114. https://doi.org/10.1016/j.jmr.2016.11.003

Chandra, K.G., Kale, D.D., 1992. Pressure-drop for laminar-flow of viscoelastic fluids in static mixers. Chem. Eng. Sci. 47, 2097–2100.

Connelly, R.K., Kokini, J.L., 2007. Examination of the mixing ability of single and twin screw mixers using 2D finite element method simulation with particle tracking. J. Food Eng. 79, 956–969. https://doi.org/10.1016/j.jfoodeng.2006.03.017

Edwards, I., Axon, S.A., Barigou, M., Stitt, E.H., 2009. Combined Use of PEPT and ERT in the Study of Aluminum Hydroxide Precipitation. Ind. Eng. Chem. Res. 48, 1019–1028. https://doi.org/10.1021/ie8010353

Faes, M., Glasmacher, B., 2008. Measurements of micro- and macromixing in liquid mixtures of reacting components using two-colour laser induced fluorescence. Chem. Eng. Sci., Model-Based Experimental Analysis 63, 4649–4655. https://doi.org/10.1016/j.ces.2007.10.036

Fu, T., Carrier, O., Funfschilling, D., Ma, Y., Li, H.Z., 2016. Newtonian and Non-Newtonian Flows in Microchannels: Inline Rheological Characterization. Chem. Eng. Technol. 39, 987–992. https://doi.org/10.1002/ceat.201500620

Hobbs, D.M., Muzzio, F.J., 1997. The Kenics static mixer: a three-dimensional chaotic flow. Chem. Eng. J. 67, 153–166. https://doi.org/10.1016/S1385-8947(97)00013-2

Jegatheeswaran, S., Ein-Mozaffari, F., Wu, J., 2018. Process intensification in a chaotic SMX static mixer to achieve an energy-efficient mixing operation of non-newtonian fluids. Chem. Eng. Process. 124, 1–10. https://doi.org/10.1016/j.cep.2017.11.018

Komzsik, L., 2003. The Lanczos Method: Evolution and Application. SIAM.

Le Guer, Y., El Omari, K., 2012. Chaotic Advection for Thermal Mixing, in: vanderGiessen, E., Aref, H. (Eds.), Advances in Applied Mechanics, Vol 45. Elsevier Academic Press Inc, San Diego, pp. 189–237.

Li, H.Z., Fasol, C., Choplin, L., 1997. Pressure Drop of Newtonian and Non-Newtonian Fluids Across a Sulzer SMX Static Mixer. Chem. Eng. Res. Des., Fluid Flow 75, 792–796. https://doi.org/10.1205/026387697524461

Machin, T.D., Wei, H.-Y., Greenwood, R.W., Simmons, M.J.H., 2018. In-pipe rheology and mixing characterisation using electrical resistance sensing. Chem. Eng. Sci. 187, 327–341. https://doi.org/10.1016/j.ces.2018.05.017

Pakzad, L., Ein-Mozaffari, F., Chan, P., 2008. Using electrical resistance tomography and computational fluid dynamics modeling to study the formation of cavern in the mixing of pseudoplastic fluids possessing yield stress. Chem. Eng. Sci. 63, 2508–2522. https://doi.org/10.1016/j.ces.2008.02.009

Paul, E.L., Atiemo-Obeng, V.A., Kresta, S.M., 2004. Handbook of Industrial Mixing: Science and Practice. John Wiley & Sons.

Peryt-Stawiarska, S., 2014. The CFD analysis of non-Newtonian fluid flow through a SMX static mixer. Przemysl Chem. 93, 196–198.

Pfund, D.M., Greenwood, M.S., Bamberger, J.A., Pappas, R.A., 2006. Inline ultrasonic rheometry by pulsed Doppler. Ultrasonics 44, E477–E482. https://doi.org/10.1016/j.ultras.2006.05.027

Pianko-Oprych, P., Nienow, A.W., Barigou, M., 2009. Positron emission particle tracking (PEPT) compared to particle image velocimetry (PIV) for studying the flow generated by a pitched-blade turbine in single phase and multi-phase systems. Chem. Eng. Sci. 64, 4955–4968. https://doi.org/10.1016/j.ces.2009.08.003

Prakash, S., Karwe, M.V., Kokini, J.L., 1999. Measurement of velocity distribution in the Brabender Farinograph as a model mixer, using Laser-Doppler Anemometry. J. Food Process Eng. 22, 435–454. https://doi.org/10.1111/j.1745-4530.1999.tb00498.x

Rafiee, M., Bakalisa, S., Fryer, P.J., Ingram, A., 2011. Study of laminar mixing in kenics static mixer by using Positron Emission Particle Tracking (PEPT). Procedia Food Sci., 11th International Congress on Engineering and Food (ICEF11) 1, 678–684. https://doi.org/10.1016/j.profoo.2011.09.102

Rahmani, R.K., Keith, T.G., Ayasoufi, A., 2005. Numerical Simulation and Mixing Study of Pseudoplastic Fluids in an Industrial Helical Static Mixer. J. Fluids Eng. 128, 467–480. https://doi.org/10.1115/1.2174058

Ramsay, J., Simmons, M.J.H., Ingram, A., Stitt, E.H., 2016. Mixing performance of viscoelastic fluids in a Kenics KM in-line static mixer. Chem. Eng. Res. Des., 10th European Congress of Chemical Engineering 115, 310–324. https://doi.org/10.1016/j.cherd.2016.07.020

Rauline, D., Le Blévec, J.-M., Bousquet, J., Tanguy, P.A., 2000. A Comparative Assessment of the Performance of the Kenics and SMX Static Mixers. Chem. Eng. Res. Des., Fluid Mixing 78, 389–396. https://doi.org/10.1205/026387600527284

Regner, M., Östergren, K., Trägårdh, C., 2006. Effects of geometry and flow rate on secondary flow and the mixing process in static mixers—a numerical study. Chem. Eng. Sci. 61, 6133–6141. https://doi.org/10.1016/j.ces.2006.05.044

Ren, Z., Kowalski, A., Rodgers, T.L., 2017. Measuring inline velocity profile of shampoo by electrical resistance tomography (ERT). Flow Meas. Instrum. 58, 31–37. https://doi.org/10.1016/j.flowmeasinst.2017.09.013

Saatdjian, E., Rodrigo, A.J.S., Mota, J.P.B., 2012. On chaotic advection in a static mixer. Chem. Eng. J. 187, 289–298. https://doi.org/10.1016/j.cej.2012.01.122

Stobiac, V., Fradette, L., Tanguy, P.A., Bertrand, F., 2014. Pumping characterisation of the maxblend impeller for Newtonian and strongly non-Newtonian fluids. Can. J. Chem. Eng. 92, 729–741. https://doi.org/10.1002/cjce.21906

Szalai, E.S., Arratia, P., Johnson, K., Muzzio, F.J., 2004. Mixing analysis in a tank stirred with Ekato Intermig® impellers. Chem. Eng. Sci. 59, 3793–3805. https://doi.org/10.1016/j.ces.2003.12.033

Uendey, C., Ertunc, S., Mistretta, T., Looze, B., 2010. Applied advanced process analytics in biopharmaceutical manufacturing: Challenges and prospects in real-time monitoring and control. J. Process Control 20, 1009–1018. https://doi.org/10.1016/j.jprocont.2010.05.008

Wageningen, W.F.C. van, Kandhai, D., Mudde, R.F., Akker, H.E.A. van den, 2004. Dynamic flow in a Kenics static mixer: An assessment of various CFD methods. AIChE J. 50, 1684–1696. https://doi.org/10.1002/aic.10178

Wang, M., Dickin, F.J., Mann, R., 1999. Electrical Resistance Tomographic Systems for Industrial Applications. Chem. Eng. Commun. 175, 49–70. https://doi.org/10.1080/00986449908912139

Wei, K., Qiu, C., Soleimani, M., Primrose, K., 2015. ITS Reconstruction Tool-Suite: An inverse algorithm package for industrial process tomography. Flow Meas. Instrum., Special issue on Tomography Measurement & Modeling of Multiphase Flows 46, 292–302. https://doi.org/10.1016/j.flowmeasinst.2015.08.001

Wunsch, O., Bohme, G., 2000. Numerical simulation of 3d viscous fluid flow and convective mixing in a static mixer. Arch. Appl. Mech. 70, 91–102. https://doi.org/10.1007/s004199900042

Yang, W.Q., Peng, L., 2003. Image reconstruction algorithms for electrical capacitance tomography. Meas. Sci. Technol. 14, R1. https://doi.org/10.1088/0957-0233/14/1/201

Yenjaichon, W., Pageau, G., Bhole, M., Bennington, C.P.J., Grace, J.R., 2011. Assessment of Mixing Quality for an Industrial Pulp Mixer Using Electrical Resistance Tomography. Can. J. Chem. Eng. 89, 996–1004. https://doi.org/10.1002/cjce.20502

Zalc, J.M., Szalai, E.S., Alvarez, M.M., Muzzio, F.J., 2002. Using CFD to understand chaotic mixing in laminar stirred tanks. AIChE J. 48, 2124–2134. https://doi.org/10.1002/aic.690481004